

# Synthesis of a New NIR Fluorescent Nd Complex Labeling Agent

Kazuki Aita · Takashi Temma · Yoichi Shimizu · Yuji Kuge · Koh-ichi Seki · Hideo Saji

Received: 15 June 2009 / Accepted: 15 September 2009 / Published online: 10 October 2009  
© Springer Science + Business Media, LLC 2009

**Abstract** Fluorescent analysis has been widely used in biological, chemical and analytical research. A useful fluorescent labeling agent should include NIR emission, a large Stoke's shift, and good labeling ability without interfering with the pharmacological profile of the labeled compound. Thus, we planned to develop an M-AMF-DOTA(Nd) derivative composed of an NIR fluorescent moiety and a maleimide conjugating moiety as a new NIR fluorescent labeling agent which fulfills these requirements. M-AMF-DOTA(Nd) was synthesized from 4-amino-fluorescein and was conjugated with an avidin molecule (Avidin-AMF-DOTA(Nd)) through Lys-side chains by reaction with 2-iminothiolane. The fluorescent features of M-AMF-DOTA(Nd) and Avidin-AMF-DOTA(Nd) were comparatively evaluated. A binding assay of Avidin-AMF-DOTA(Nd) with D-biotin and a tumor cell-uptake study were performed to estimate the effects of conjugation on the biological and physicochemical features of the protein. M-AMF-DOTA(Nd) was obtained in 22% overall yield. M-AMF-DOTA(Nd) had a typical NIR fluorescence from the Nd ion (880 nm and 900 nm from 488 nm

excitation). Avidin-AMF-DOTA(Nd) was easily synthesized and also had typical NIR fluorescence from the Nd ion without loss of fluorescent intensity. The binding affinity of Avidin-AMF-DOTA(Nd) to D-biotin was equivalent to naive avidin. Avidin-AMF-DOTA(Nd) was taken up by tumor cells in the same manner as avidin conjugated with fluorescein isothiocyanate, an established, widely used fluorescent avidin. Results from this study indicate that M-AMF-DOTA(Nd) is a potential labeling agent for routine NIR fluorescent analysis.

**Keywords** Neodymium · Near-infrared · Fluorescent labeling · Maleimide

## Introduction

Fluorescent imaging, one of several molecular imaging techniques, is a very convenient method because of its simple and safe operation, high spatial resolution, and short detection time. Fluorescent labels are widely used for applications in biology [1], biotechnology [2], medicine [3], and in combinatorial chemistry [4] as encoders of individual library members and as reporters of chemical reactions. Fluorescent labeling agents should not influence the pharmacological character of a labeled compound. In addition, near-infrared (NIR) fluorescence and a large Stoke's shift are desirable characteristics of labeling agents in the fields of biology, biotechnology, and medicine since NIR light has good permeability in living organisms and there is negligible self-fluorescence in the NIR region. A large Stoke's shift makes it easier to remove scattered and reflected excitation light by suitable optical filters. However, there are few agents that possess all of these features. Thus, we planned to develop a novel

---

K. Aita · T. Temma · Y. Shimizu · Y. Kuge · H. Saji (✉)  
Department of Patho-Functional Bioanalysis,  
Graduate School of Pharmaceutical Sciences, Kyoto University,  
Kyoto, Japan  
e-mail: hsaji@pharm.kyoto-u.ac.jp

K. Aita · K. Seki  
Central Institute of Isotope Science, Hokkaido University,  
Sapporo, Hokkaido, Japan

Y. Kuge  
Department of Tracer Kinetics & Bioanalysis,  
Graduate School of Medicine, Hokkaido University,  
Sapporo, Hokkaido, Japan

fluorescent labeling agent for fluorescent imaging of proteins in living organisms.

We recently reported new NIR fluorescent dyes with low molecular weight, 4AMF-DOTA(Nd) (MW=883) [5] and PAN-DOTA(Yb) (MW=823) [6], which include lanthanide complexes in their structures. They had NIR emission and large Stoke's shifts (880 and 900 nm from 488 nm excitation light for 4AMF-DOTA(Nd), 975 nm from 530 nm excitation light for PAN-DOTA(Yb)). Their emission wavelengths were constant under various conditions (pH and solvents). Therefore, these NIR fluorescent dyes are promising candidates for use as fluorescent labeling agents with some modification. In this regard, we selected 4AMF-DOTA(Nd) as the starting structure of the labeling agent because it has several functional groups capable of being modified to bind with a functional molecule and at the excitation wavelength it has a stronger absorption and gives a more potent signal intensity than PAN-DOTA(Yb).

A conjugating moiety was required to link 4AMF-DOTA (Nd) and a functional molecule. As a conjugating moiety, maleimide was selected because it has very fast reactivity, good selectivity, and makes a very stable bond with thiols. Maleimide was linked to one of the DOTA carboxyl groups [7], and the remaining carboxyl groups were capped as amides in order to avoid changes in fluorescence and chelating ability since carboxyl groups often interact with cationic groups and solutes which might alter the fluorescence properties of the complex. The selection of a suitable spacer between the fluorophore and the conjugation moiety is also important. We selected a 6-atom ethyl-propyl amide chain as the spacer because moderately inflexible chains composed of 6~12 atoms have been adopted as an appropriate length and rigidity to suppress interaction between the labeled molecule and the fluorophore, which otherwise could result in altered fluorescence as well as chemical and physical properties of the labeled molecule [8–12].

The above analysis led to the design and synthesis of M-AMF-DOTA(Nd) that includes a maleimide (Scheme 1) as a new NIR fluorescent labeling agent with a large Stoke's shift. In addition, we have evaluated the imaging potential of M-AMF-DOTA(Nd) conjugated to avidin (Avidin-AMF-DOTA(Nd)) through binding experiments with biotin and in tumor cell-uptake studies.

## Materials and methods

### Materials

All chemicals used in this study were commercial products of the highest purity and if necessary were further purified

by standard methods. Avidin and D-biotin were purchased from Nacalai Tesque, Inc. (Kyoto, Japan).  $^{125}\text{I}$ -iodide was purchased from Perkin Elmer Life and Analytical Sciences (Boston, MA). C6 glioma cells were purchased from the Health Science Research Resources Bank (Tokyo, Japan).

### Instruments

FT-IR spectra were recorded with a Shimadzu, IRAffinity-1 (Shimadzu Corporation, Kyoto, Japan). UV-vis spectra were measured using a UV-1800 (Shimadzu Corporation, Kyoto, Japan). ESI-MS measurements were performed on a Shimadzu LC-MS2010 EV (Shimadzu Corporation, Kyoto, Japan).  $^1\text{H}$ -NMR spectra were recorded on a JEOL JNM-AL400 (JEOL Ltd., Tokyo, Japan). Fluorescent spectroscopy was performed with a Fluorolog-3 with a NIR sensitive photomultiplier detection system (~1200 nm) (HORIBA Jobin Yvon Inc., Kyoto, Japan). The slit width was 10 nm for both excitation and emission measurements. Time-resolved fluorescence spectra were recorded on a Fluorolog-3 with Phosphorescence (HORIBA Jobin Yvon Inc., Kyoto, Japan). The slit width was 12 nm for both excitation and emission. In both fluorescence spectra measurements, the photomultiplier voltage was 1450 V. Flow cytometry was performed on a FACScan (Becton Dickinson Inc., Franklin Lakes, NJ, USA). Radioactivities were counted by Cobra Auto-Gamma Counter 5010 (Packard instruments Co., Downers Grove, IL, USA). Fluorescent images were photographed with a ChemiDoc XRS (Bio-Rad Japan, Tokyo, Japan).

### Fluorescence emission and excitation spectral measurements

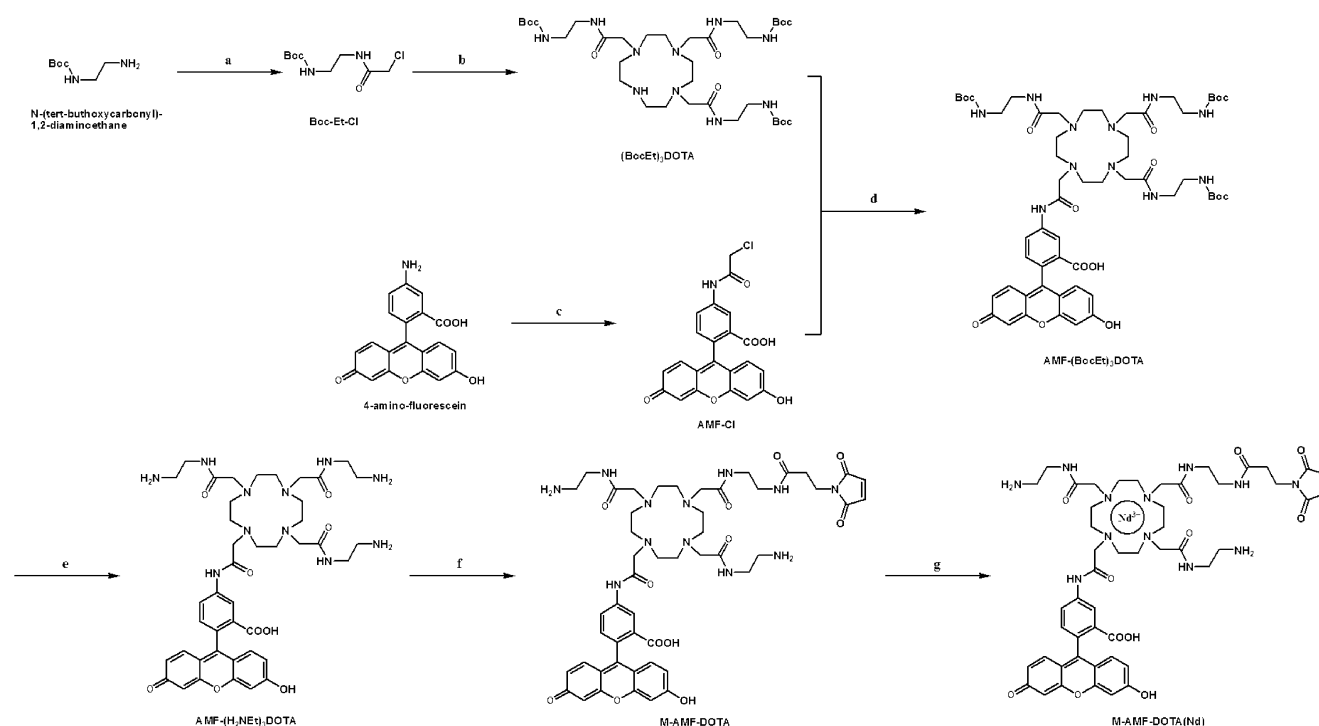
The fluorescence emission spectra of M-AMF-DOTA(Nd), M-AMF-DOTA, Avidin-AMF-DOTA(Nd), and 4AMF-DOTA(Nd) (10  $\mu\text{M}$ ) were measured in 10 mM Tris-HCl buffer (pH 8.0) at 25 °C, following excitation at 488 nm.

### UV-visible absorption spectral measurements

The absorption spectral changes of AMF-DOTA(Nd), M-AMF-DOTA and M-AMF-DOTA(Nd) (10  $\mu\text{M}$ ) in 10 mM Tris-HCl buffer (pH 8.0) at 25 °C were determined.

### Quantum yield analysis

Quantum yield analyses of M-AMF-DOTA(Nd) and 4AMF-DOTA(Nd) were measured by a previously reported method [13] in 10 mM Tris-HCl buffer (pH 8.0) at 25 °C, following excitation at 488 nm and emission at 880 nm. The reference compound,  $[\text{Yb}(\text{Tropolonate})_4]$ , was measured at 380 nm excitation and 975 nm emission in 10 mM



**Scheme 1** Synthetic scheme of M-AMF-DOTA(Nd). Reagents and conditions: **a**) chloroacetyl chloride, 0 °C, 3 h, **b**) cyclen 4HCl,  $^i\text{Pr}_2\text{EtN}$ , 80 °C, 9 h, **c**) chloroacetyl chloride, 0 °C, 1 h, **d**)  $\text{K}_2\text{CO}_3$ ,

80 °C, 7 h, **e**) TFA, 0 °C, 10 min, **f**) N-succinimidyl-3-maleimidepropionate,  $\text{Et}_3\text{N}$ , room temperature, 1 h, **g**)  $\text{NdCl}_3 \cdot 6\text{H}_2\text{O}$

Tris-HCl buffer. The absorbance of the samples was adjusted to not exceed 0.2 at the excitation wavelength. The wavelength dependence on excitation light intensity and the detection efficiency of emission light were as given from HORIBA Jobin Yvon Inc.

#### Time-delayed fluorescence spectral measurement

The time-delayed fluorescence spectra of M-AMF-DOTA(Nd) (10  $\mu\text{M}$ ) were measured in 10 mM Tris-HCl buffer (pH 8.0) at 25 °C, following excitation at 488 nm. A delay time of 7  $\mu\text{s}$  and a gate time of 100  $\mu\text{s}$  were used.

#### Fluorescence lifetime measurements

The fluorescence lifetime of M-AMF-DOTA(Nd) (10  $\mu\text{M}$ ) in 10 mM Tris-HCl buffer (pH 8.0) at 25 °C was determined. The data, obtained by monitoring the emission intensity at 880 nm ( $\lambda_{\text{ex}}=488$  nm), were collected at a resolution of 1  $\mu\text{s}$  and were fit to a single-exponential curve using the equation shown below (Eq. 1), where  $I_0$  and  $I$  are the fluorescence intensities at time  $t=0$  and time  $t$ , respectively, and  $\tau$  is the fluorescence emission lifetime.

$$I = I_0 \exp(-t/\tau) \quad (1)$$

#### Biotin competitive assay

[ $^{125}\text{I}$ ]-IBB ([ $^{125}\text{I}$ ]-3-iodobenzoyl)norbiotinamide) was prepared as previously described [14]. [ $^{125}\text{I}$ ]-IBB (0.5 mCi/mL) 10  $\mu\text{L}$ , D-biotin (5, 50, 500, 1000 mM) 100  $\mu\text{L}$ , and PBS 290  $\mu\text{L}$  were added to a microtube containing 100  $\mu\text{L}$  of Avidin-AMF-DOTA(Nd) (80  $\mu\text{g}/\text{mL}$ ) or avidin (80  $\mu\text{g}/\text{mL}$ ). The reaction was performed at 37 °C for 1 h. The reaction mixture was applied to an Amicon Microcon filter (Millipore) and centrifuged at 4 °C,  $1467 \times g$  for 30 min (Micro Cooling Centrifuge 1720, Kubota, Osaka, Japan). The radioactivities of the reactant and filtrate were then measured, and the binding rate was calculated.

#### Cellular uptake study of Avidin-AMF-DOTA(Nd) and Avidin-FITC

C6 glioma cells were maintained at 37 °C in a humidified atmosphere containing 5%  $\text{CO}_2$  in Dulbecco's modified eagle medium (DMEM) and 10% fetal bovine serum. Avidin-AMF-DOTA(Nd) or avidin conjugated to fluorescein isothiocyanate (Avidin-FITC) (50  $\mu\text{g}/\text{mL}$  in DMEM, 1.0 mL) were added to C6 glioma cells ( $1 \times 10^5$  cells/dish) and incubated for 1, 3, or 6 h. After incubation, the cells were twice washed with PBS(-), and then treated with trypsin to release them from the dish. Fluorescence levels were

measured using a flow cytometer. Fluorescence intensities were normalized for quantum yield ( $\varphi=0.21$  and  $0.60$  for Avidin-AMF-DOTA(Nd) and Avidin-FITC, respectively) and the number of labeling agents ( $2.5$  and  $4.0$  for Avidin-AMF-DOTA(Nd) and Avidin-FITC, respectively).

### Synthesis

4-(Chloromethylamide)fluorescein (4AMF-Cl) [5] and radiolabeled IBB ( $[^{125}\text{I}]\text{-IBB}$ ) [14] were prepared as previously described.

N-tert-butoxycarbonyl-2-(2-chloroacetoamide)-aminoethane (Boc-Et-Cl)

To a  $\text{CHCl}_3$  solution (100 mL) of N-(tert-butoxycarbonyl)-1,2-diaminoethane (1.60 g, 10 mmol) and  $\text{Et}_3\text{N}$  (10.1 g, 100 mmol) was slowly added  $\text{ClCH}_2\text{COCl}$  (1.13 g, 10 mmol) in  $\text{CHCl}_3$  solution (20 mL) at  $0^\circ\text{C}$ . The solution was stirred for 3 h and then evaporated to remove the solvent. The black-yellow residue was purified by silica gel column chromatography to obtain Boc-Et-Cl as a pale yellow powder (2.0 g, 8.5 mmol, 85%)

LR-MS(ESI, neg.)  $m/z$  found 237 ( $[\text{M}+\text{H}]^+$ ), calcd. 237

HR-MS (FAB, pos.)  $m/z$  found 237.0928, calcd. 237.0928 ( $\text{C}_9\text{H}_{18}\text{ClN}_2\text{O}_3$ )

$^1\text{H-NMR}$  (400 MHz,  $\text{CDCl}_3$ )  $\delta$  4.83 (2H, s), 3.46 (2H, t,  $J=7.3$  Hz), 3.25 (2H, t,  $J=7.3$  Hz), 1.45 (9H, s)

1,4,7-tris(2-(tert-butoxycarbonyl)-2-aminoethylamidemethyl)-1,4,7,10-tetraazacyclododecane ((BocEt) $_3$ DOTA)

To a dry MeCN solution (50 mL) of 1,4,7,10-tetraazacyclododecane tetrahydrochloride (cyclen 4HCl) (318 mg, 1.0 mmol),  $^1\text{Pr}_2\text{EtN}$  (1.3 g, 10.0 mmol) was added, and the reaction was stirred for 5 min at  $40^\circ\text{C}$  under anaerobic conditions. Then Boc-Et-Cl (708 mg, 3 mmol) in dry MeCN solution (10 mL) was slowly added to the suspension. After stirring for 9 h at  $80^\circ\text{C}$ , the solution was evaporated to remove the solvent. The pale yellow residue was purified by silica gel column chromatography to obtain (BocEt) $_3$ DOTA as a white powder (320 mg, 0.4 mmol, 41%)

LR-MS(ESI, neg.)  $m/z$  found 774 ( $[\text{M}+\text{H}]^+$ ), calcd. 774

HR-MS (FAB, pos.)  $m/z$  found 773.5171 calcd. 773.5171 ( $\text{C}_{32}\text{H}_{62}\text{N}_{10}\text{O}_9$ )

$^1\text{H-NMR}$  (400 MHz,  $\text{CD}_3\text{OD}$ )  $\delta$  3.52–2.64 (34H, m), 1.50 (27H, s)

1-(4-Amidemethyl-fluorescein)-4,7,10-tris(2-(tert-butoxycarbonyl)-2-aminoethylamidemethyl)-1,4,7,10-tetraazacyclododecane (AMF-(BocEt) $_3$ DOTA)

A dry DMF solution (10 mL) of (BocEt) $_3$ DOTA (150 mg, 0.2 mmol) and  $\text{K}_2\text{CO}_3$  (0.7 g, 5.0 mmol) was stirred for 5 min at  $80^\circ\text{C}$  under anaerobic conditions. To the solution was slowly added 4-AMF-Cl (85 mg, 0.2 mmol) in dry DMF solution (10 mL). After stirring for 7 h at  $80^\circ\text{C}$ , the solution was evaporated to remove the solvent. The resulting residue was redissolved in a minimum amount of MeOH, the solution was poured into  $\text{Et}_2\text{O}$  (20 mL), and the resulting residue was washed three times with  $\text{Et}_2\text{O}$  by decantation. The powder was dried under vacuum to obtain AMF-(BocEt) $_3$ DOTA (139 mg, 0.14 mmol, 60%) as a red powder.

LR-MS(ESI, pos.)  $m/z$  found 1161 ( $[\text{M}+\text{H}]^+$ ), calcd. 1161

HR-MS (FAB, pos.)  $m/z$  found 1160.5914 calcd. 1160.5914 ( $\text{C}_{57}\text{H}_{82}\text{N}_{11}\text{O}_{15}$ )

$^1\text{H-NMR}$  (400 MHz,  $\text{CD}_3\text{OD}$ )  $\delta$  8.38 (1H, s), 7.91 (1H, d,  $J=7.3$  Hz), 6.62 (3H, m), 6.52 (2H, s), 6.44 (2H, dd,  $J=1.9, 8.7$  Hz), 3.51–2.66 (36H, m), 1.42 (27H, s)

1-(4-Amidemethyl-fluorescein)-4,7,10-tris(2-aminoethylamidemethyl)-1,4,7,10-tetraazacyclododecane (AMF-( $\text{H}_2\text{NEt}$ ) $_3$ DOTA)

TFA (2.0 mL) was slowly added to a MeOH solution of AMF-(BocEt) $_3$ DOTA (116 mg, 0.1 mmol) at  $0^\circ\text{C}$ . The solution was stirred for 10 min, and the mixture was evaporated to remove the solvent. The resulting residue was redissolved in a minimum amount of MeOH and evaporated. This procedure was repeated three times. The resulting powder was dried under vacuum to obtain AMF-( $\text{H}_2\text{NEt}$ ) $_3$ DOTA (85 mg, 0.1 mmol, 99%) as an orange powder.

LR-MS(ESI, pos.)  $m/z$  found 860 ( $[\text{M}+\text{H}]^+$ ), calcd. 860

HR-MS (FAB, pos.)  $m/z$  found 860.4341 calcd. 860.4341 ( $\text{C}_{42}\text{H}_{58}\text{N}_{11}\text{O}_9$ )

$^1\text{H-NMR}$  (400 MHz,  $\text{CD}_3\text{OD}$ )  $\delta$  8.38 (1H, s), 7.91 (1H, d,  $J=7.3$  Hz), 6.62 (3H, m), 6.52 (2H, s), 6.44 (2H, dd,  $J=1.9, 8.7$  Hz), 3.53–2.62 (36H, m)

1-(4-Amidemethyl-fluorescein)-4,10-di(2-aminoethylamidemethyl)-7-(2-(3-maleimidopropionate)-2-aminoethylamidemethyl)-1,4,7,10-tetraazacyclododecane (M-AMF-DOTA)

To a dry DMF solution (10 mL) of AMF-( $\text{H}_2\text{NEt}$ ) $_3$ DOTA (85 mg, 0.1 mmol) and  $\text{Et}_3\text{N}$  (100 mg, 1.0 mmol) was added N-succinimidyl-3-maleimidepropionate (26 mg,

0.1 mmol), and the reaction was stirred for 1 h at room temperature under anaerobic conditions. The solution was evaporated to remove the solvent. The resulting residue was redissolved in a minimum amount of MeOH. The solution was poured in Et<sub>2</sub>O (5 mL), and the resulting residue was washed three times with Et<sub>2</sub>O by decantation. The powder was dried under vacuum to obtain M-AMF-DOTA (55 mg, 0.05 mmol, 55%) as a red powder.

LR-MS(ESI, neg.) *m/z* found 504 ([M-2H]<sup>2-</sup>), calcd. 504

HR-MS (FAB, neg.) *m/z* found 1009.4610 calcd. 1009.4610 (C<sub>49</sub>H<sub>61</sub>N<sub>12</sub>O<sub>12</sub>)

<sup>1</sup>H-NMR (400 MHz, CD<sub>3</sub>OD) δ 8.38 (1H, s), 7.91 (1H, d, *J*=7.3 Hz), 6.62 (3H, m), 6.52 (2H, s), 6.92 (2H, d, *J*=7.3 Hz), 6.44 (2H, dd, *J*=1.9, 8.7 Hz), 3.51–2.43 (40H, m)

#### M-AMF-DOTA(Nd)

To an EtOH solution (10 mL) of M-AMF-DOTA (10.1 mg, 10 μmol) was added NdCl<sub>3</sub>·6H<sub>2</sub>O (3.6 mg, 10 μmol). After stirring for 1 h at room temperature in the dark, the reaction mixture was filtered. The filtrate was evaporated and dried in vacuo to obtain M-AMF-DOTA(Nd) (10.4 mg, 9.0 μmol, 90%) as a red powder.

LR-MS (ESI, pos.) *m/z* found 576 ([M-H]<sup>2+</sup>), calcd. 576

HR-MS (FAB, pos.) *m/z* found 1150.3531 calcd. 1150.3531 (C<sub>49</sub>H<sub>60</sub>N<sub>12</sub>NdO<sub>12</sub>)

#### Avidin-AMF-DOTA(Nd)

To avidin (1.0 mg, 15 nmol) in borate buffer (0.16 M with 2 mM EDTA, 100 μL) was added 2-iminothiolane (255 μg, 185 nmol) in borate buffer (0.16 M with 2 mM EDTA, 25.5 μL). After incubation at room temperature for 1 h, dithiothreitol (30.8 μg, 2.0 μmol) in H<sub>2</sub>O (2.0 μL) was added to the reaction mixture, and the reaction was allowed to stand for 15 min. After purification of the thiolated avidin by spin-column (Sephadex G50, GE healthcare UK Ltd.), a solution of PBS (0.1 M, pH 7.4, 172 μL) containing M-AMF-DOTA(Nd) (1.7 mg, 1.5 μmol) was added. The mixture was incubated at 37 °C for 1 h in the dark. After incubation, N-ethyl maleimide (40 μg, 32 nmol) in DMSO (4.0 μL) was added to cap unreacted thiols and the reaction was further incubated at room temperature for 30 min in the dark. After size-exclusion filtration twice with a PD-10 column (17-0851-01, GE Healthcare UK Ltd.) using 0.1 M PBS (pH 7.4), Avidin-AMF-DOTA(Nd) was obtained.

The fluorescence spectrum of Avidin-AMF-DOTA(Nd) was measured by Fluorolog-3. The progress of the labeling

reaction was confirmed by electrophoresis. Avidin-AMF-DOTA(Nd) and Avidin-AMF-DOTA were denatured in PBS by heating at 100 °C for 5 min. Then samples (10 μL in each well) were separated by one-dimensional denaturing sodium dodecyl sulfate-polyacrylamide gel electrophoresis (SDS-PAGE) with a 5% to 20% gradient polyacrylamide gel (ePAGEL E-T520L, ATTO). A standard marker (Precision Plus Protein<sup>TM</sup> Standards, BIO-RAD) was used as a protein molecular weight marker. After electrophoresis using the AE-8155 myPower-II 500 (ATTO) at 400 V, 20 mA for 70 min, the gel was stained with Coomassie Brilliant Blue R250 (CBB) to visualize the proteins.

The number of thiols introduced per avidin was calculated by the following method: 4,4'-dithiodipyridine (22 μg in 0.1 M PBS (pH 7.4, 20 μL)) was added to thiolated avidin (85 μg in 0.1 M PBS (pH 7.4, 500 μL)), and the reaction was incubated at 30 °C for 30 min. After incubation, the absorbances of the reaction mixture at 280 nm and 324 nm were measured to calculate the number of thiols ( $\epsilon=113,900, 7,060$  for avidin and thiol, respectively) using the equation below (Eq. 2).

$$\text{Number of thiol} = \frac{(A_{342}/\epsilon_{\text{thiol}})}{A_{280}/\epsilon_{\text{avidin}}} \quad (2)$$

The number of M-AMF-DOTA(Nd) and M-AMF-DOTA per avidin were calculated by the equation below (Eq. 3) using the absorbances measured at 280 and 488 nm of Avidin-AMF-DOTA(Nd) or Avidin-AMF-DOTA ( $\epsilon=113,900, 18,000$  and  $18,000$  L/(M\*cm) for avidin, AMF-DOTA(Nd) and AMF-DOTA, respectively).

$$\text{Number of dye} = \frac{(A_{488}/\epsilon_{\text{dye}})}{(A_{280}/\epsilon_{\text{avidin}})} \quad (3)$$

#### Avidin-FITC

To avidin (1.1 μg, 17 nmol) in 20 mM Na<sub>2</sub>HPO<sub>4</sub> (aq) (112 mL) was added FITC-I (126 μg, 322 nmol) in DMSO (12.6 μL). The mixture was incubated at room temperature for 1 h in the dark. After incubation, the mixture was purified by size-exclusion filtration with a PD-10 column (17-0851-01, GE Healthcare UK Ltd.) using 0.1 M PBS (pH 7.4) to obtain Avidin-FITC.

The fluorescence of Avidin-FITC was measured by Fluorolog-3. SDS-PAGE and CBB staining of Avidin-FITC were performed by the same methods as for Avidin-AMF-DOTA. The number of FITC groups introduced onto avidin was calculated by the same method as for Avidin-AMF-DOTA ( $\epsilon=113,900$  and  $80,000$  L/(M\*cm) for avidin and FITC (488 nm), respectively).

## Results

### Synthesis and characterization of M-AMF-DOTA(Nd)

M-AMF-DOTA was synthesized from 4-amino-fluorescein and cyclen in six steps as shown in Scheme 1. The overall yield from 4-aminofluorescein was 24%. M-AMF-DOTA (Nd) was easily synthesized in 90% yield by stirring M-AMF-DOTA and NdCl<sub>3</sub> in MeOH.

In the IR spectra, amide-I absorptions were observed at 1558 cm<sup>-1</sup> for M-AMF-DOTA and 1571 cm<sup>-1</sup> for M-AMF-DOTA(Nd), and amide-II absorptions were found at 1635 cm<sup>-1</sup> for M-AMF-DOTA and 1651 cm<sup>-1</sup> for M-AMF-DOTA(Nd) (data not shown).

The UV-vis absorption spectra of M-AMF-DOTA(Nd), M-AMF-DOTA and 4AMF-DOTA(Nd) in buffer are shown in Fig. 1A. Each spectrum shows the same strong absorption peak at 490 nm.

The emission spectra of M-AMF-DOTA(Nd), M-AMF-DOTA and 4AMF-DOTA(Nd) in buffer are shown in Fig. 1B. Typical characteristic peaks at 880 nm and 900 nm were detected in the M-AMF-DOTA(Nd) and 4AMF-DOTA(Nd) spectra ( $\lambda_{\text{ex}}=488$  nm). In contrast, characteristic fluorescence peaks were not detected for M-AMF-DOTA under the same conditions. The 880 nm and 900 nm emission signals for M-AMF-DOTA(Nd) were slightly stronger than for 4AMF-DOTA(Nd). The quantum yields of M-AMF-DOTA(Nd) and 4AMF-DOTA(Nd) were calculated to be  $1.2 \times 10^{-5}$  and  $4.5 \times 10^{-6}$ , respectively.

The excitation spectra of M-AMF-DOTA(Nd), M-AMF-DOTA and 4AMF-DOTA(Nd) in buffer are shown in Fig. 1C ( $\lambda_{\text{em}}=880$  nm for M-AMF-DOTA(Nd) and 4AMF-DOTA(Nd) or 515 nm for M-AMF-DOTA). Each spectrum shows the same excitation peak at 490 nm.

### Long-lived fluorescence measurement of M-AMF-DOTA (Nd)

Time-resolved fluorescence (TRF) measurements of M-AMF-DOTA(Nd) are shown in Fig. 2. Although a tailing fluorescence signal from the fluorescein moiety was detected below 850 nm in addition to the fluorescence from Nd at 880 and 900 nm in the emission spectrum without TRF measurement, the fluorescence from fluorescein was not observed in the emission spectrum with TRF measurement. Furthermore, we calculated the lifetime of Nd ion fluorescence using the equation described in the Experimental section. The calculated lifetime was 2.3  $\mu\text{s}$  for the 880 nm fluorescence.

### Synthesis and characterization of Avidin-AMF-DOTA(Nd)

The number of AMF-DOTA(Nd) and AMF-DOTA per avidin molecule were approximately 2.5 and 5.0, respectively.

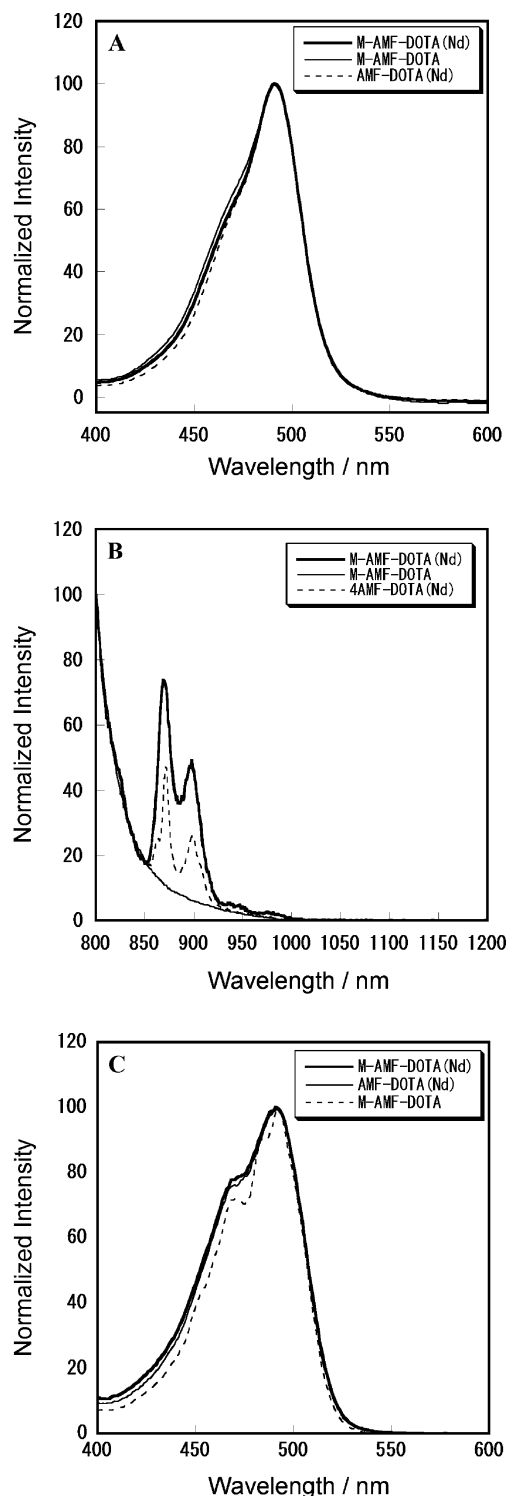


**Fig. 1** Spectroscopy data for M-AMF-DOTA(Nd) (*bold line*), M-AMF-DOTA (*solid line*) and 4AMF-DOTA(Nd) (*dotted line*). **A** UV-vis absorption spectra **B** Emission spectra ( $\lambda_{\text{ex}}=488$  nm). **C** Excitation spectra ( $\lambda_{\text{em}}=880$  nm for M-AMF-DOTA(Nd) and 4AMF-DOTA(Nd), 515 nm for M-AMF-DOTA)

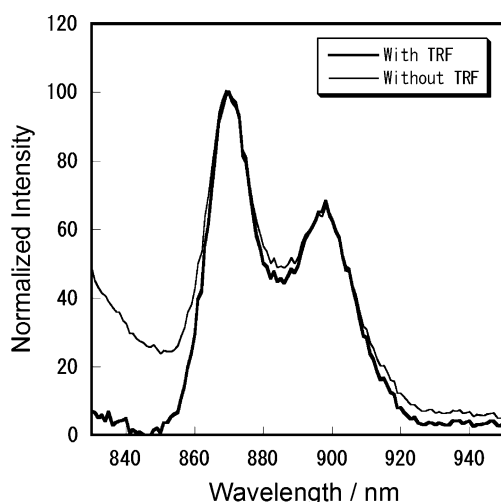


**Fig. 2** Emission spectra of M-AMF-DOTA(Nd) with (*bold line*) and without (*narrow line*) time-resolved fluorescence (TRF) measurement

In the SDS-PAGE analysis of purified Avidin-AMF-DOTA(Nd), the avidin mono-subunit (17 kDa) band was clearly observed (Fig. 3). This band exhibited fluorescence in the 548~630 nm region from 302 nm excitation. The emission spectra of aqueous solutions of Avidin-AMF-DOTA(Nd) and M-AMF-DOTA(Nd) are shown in Fig. 4. Typical characteristic peaks, the same as for M-AMF-DOTA(Nd), at 880 nm and 900 nm were detected in the Avidin-AMF-DOTA(Nd) spectrum ( $\lambda_{\text{ex}}=488$  nm).

#### Biotin binding assay of Avidin-AMF-DOTA(Nd)

The binding ability of Avidin-AMF-DOTA(Nd) to D-biotin was estimated by a displacement assay in comparison with avidin (Fig. 5). The binding of Avidin-AMF-DOTA(Nd) toward radiolabeled biotin was inhibited by D-biotin in a dose-dependent manner. Avidin-AMF-DOTA(Nd) and avidin showed similar displacement curves.

#### Cellular uptake study of Avidin-AMF-DOTA(Nd)

Figure 6 shows the normalized fluorescence intensity of C6 glioma cells incubated with Avidin-AMF-DOTA(Nd) and

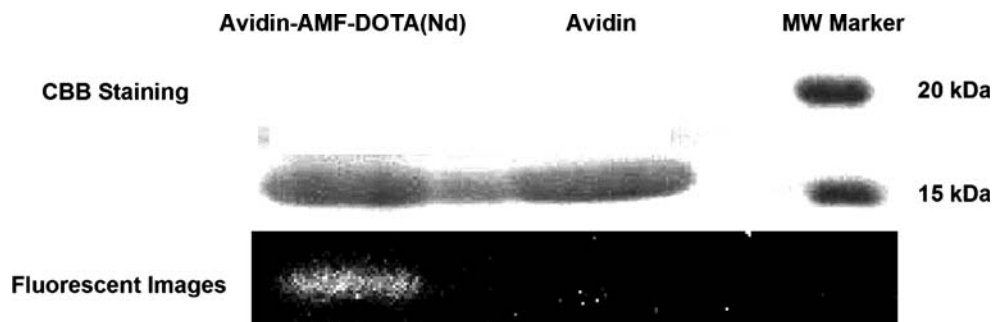
Avidin-FITC. In the cellular uptake study, Avidin-AMF-DOTA(Nd) and Avidin-FITC displayed similar time-dependent increases in fluorescence intensity after normalization by quantum yield and number of labeling agents. Cellular appearance did not change during the incubation.

#### Discussion

There are some requirements that an ideal fluorescent labeling agent should fulfill. First, the label needs to emit fluorescence in a region that does not overlap with other light derived from the excitation or other compounds in test tubes, solutions, organs, or cells [15,16]. A non-desired overlap could lead to a decrease in the signal-to-noise ratio. Second, fluorescence properties should not be changed by conjugation with a functional molecule for an accurate evaluation in subsequent studies. A change in the emission wavelength after conjugation would make interpretation of the data complex. Third, the ideal labeling agent should be able to label various compounds in an easy, quantifiable operation. Lastly, the fluorescent agent should not affect the chemical, physical, and biological features of the labeled compound after conjugation. The results obtained in this study indicate that M-AMF-DOTA(Nd) fulfilled all of the above requirements.

M-AMF-DOTA was easily synthesized by standard methods. For the introduction of maleimide to M-AMF-DOTA by amidation (Scheme 1, step f), the concentration of the reactants was very important. For the reaction conducted at a 10 mM concentration, only the 7-position amide M-AMF-DOTA was isolated; 4- and 10-position amide isomers were not observed. However, for reactions conducted at concentrations of 20~50 mM, 4- or 10-position isomers and di-maleimide products were observed. M-AMF-DOTA(Nd) displayed characteristic emission peaks at 880 nm and 900 nm (Fig. 1B,  $\lambda_{\text{ex}}=488$  nm) which can be assigned to a typical Nd  $^4F_{3/2}$  to  $^4I_{9/2}$  transition, the same as 4AMF-DOTA(Nd) [5]. The quantum yield of M-AMF-DOTA(Nd) was approximately 2.5 times higher than that of 4AMF-DOTA(Nd). This might be caused

**Fig. 3** CBB staining and Fluorescent images of Avidin-AMF-DOTA(Nd) and avidin



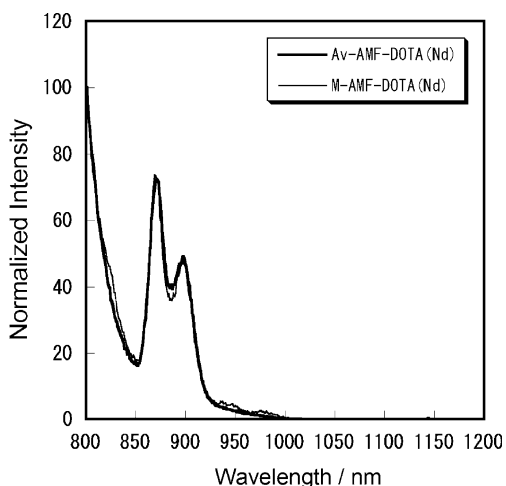


**Fig. 4** Fluorescence spectra of Avidin-AMF-DOTA(Nd) (*bold line*) and M-AMF-DOTA(Nd) (*narrow line*). Each spectrum was measured with 488 nm excitation

by the DOTA modification, aminoethylation of the carboxylic acid, which hinders the approach of fluorescent quenchers ( $\text{H}_2\text{O}$  etc.) to the Nd ion in M-AMF-DOTA(Nd). In addition, the fluorescence lifetime of 2.3  $\mu\text{s}$  for the Nd complex was in agreement with previous reports [17,18]. Although the fluorescence of fluorescein and the Nd ion were observed without TRF measurements, fluorescein fluorescence was not observed in the emission spectra with TRF measurement resulting in extraction of only fluorescence from Nd. Therefore, TRF measurement is a potentially useful method for compounds labeled by M-AMF-DOTA(Nd).

UV-vis spectra of buffer solutions of M-AMF-DOTA (Nd), M-AMF-DOTA and 4AMF-DOTA(Nd) showed the same absorption shape assigned to fluorescein absorption. This result suggests that the modification of DOTA and the chelation of the Nd ion to DOTA derivatives have no effect

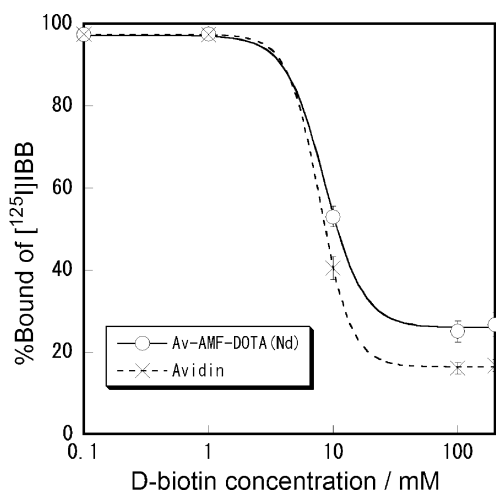


**Fig. 5** Displacement assay of Avidin-AMF-DOTA(Nd) (*solid line*) (or avidin (*dotted line*)), [ $^{125}\text{I}$ ]-IBB and various concentrations of D-biotin

on the energy level of the fluorescein moiety. The excitation spectra of M-AMF-DOTA(Nd) ( $\lambda_{\text{em}}=880$  nm) and M-AMF-DOTA ( $\lambda_{\text{em}}=515$  nm) showed much the same features (Fig. 1C). Thus, the supposition that the fluorescence of M-AMF-DOTA(Nd) at 880~900 nm is derived from the transfer of energy from an excited fluorescein moiety, the same as in the case of 4AMF-DOTA(Nd) [5], is supported by the data.

NIR fluorescence analysis is particularly suited to living organisms because they contain few fluorescent compounds in the NIR region (700~1000 nm) while there are many naturally occurring fluorescent compounds in the visible region, such as fluorite (400~600 nm) [19], anthracene (400 nm), chlorophyll (680 nm) [20], NAD(P)H (450 nm) [21] and flavin (520 nm) [22]. Thus, NIR fluorescent dyes are recognized to be useful for fluorescent analysis [23–25]. In addition, fluorescence from lanthanides has a significant advantage in that the wavelength is constant with changes in environmental factors (solvent, pH, etc.) [6]. This is derived from the mechanism of lanthanide fluorescence where the 4f orbital responsible for fluorescence is located inside the 5 s and 5 d orbitals, which protect the fluorescence from environmental effects. A very large Stoke's shift for M-AMF-DOTA(Nd) (about 400 nm) is another advantage over most other organic fluorescent labels. This contributes to the easy separation of the emission signals from the excitation light by suitable optical filters. Although to date there are few instruments with good imaging ability in the NIR region (especially 800~1200 nm), NIR fluorescent analysis using potential labeling agents such as M-AMF-DOTA(Nd) could be effective with the development of suitable imaging instruments.

Thiolated avidin was easily labeled by M-AMF-DOTA (Nd). The number of AMF-DOTA(Nd) complexes per avidin was half that of AMF-DOTA under the same

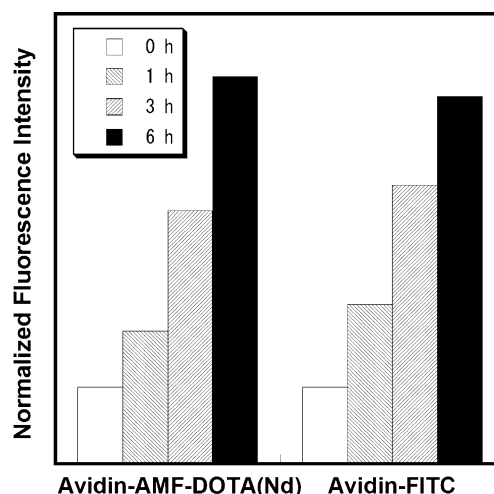


**Fig. 6** Normalized fluorescence intensity of C6 glioma cells incubated with Avidin-AMF-DOTA(Nd) (*left*) or Avidin-FITC (*right*)



reaction conditions, which would seem to be caused by a difference in tertiary structure. It is well known that lanthanide-DOTA derivative complexes form cage-like structures [26–28]. Therefore, M-AMF-DOTA(Nd) is a more rigid and hindered structure compared with M-AMF-DOTA. Thus, the maleimide group of M-AMF-DOTA(Nd) as compared with M-AMF-DOTA would have less chance of approaching a thiol group. It is remarkable that M-AMF-DOTA(Nd) is still reactive enough for the following studies as shown in Figs. 3, 4, 5, and 6.

Since maleimides readily react with thiols, we labeled avidin through Lys side chain  $\text{NH}_2$  groups via conversion to thiols by reaction with 2-iminothiolane. This intermediate step is necessary because all Cys side chains in avidin form disulfide bonds [29] while most of the Lys side chains (about 6 or 7 per avidin monomer) are free on the protein surface [29]. The labeling reaction was easily completed, which demonstrates that the M-AMF-DOTA(Nd) fluorescent labeling agent could be linked with proteins through not only thiol but also primary amine side chains.

In a displacement assay, both Avidin-AMF-DOTA(Nd) and naive avidin were inhibited by D-biotin in a similar dose-dependent manner (Fig. 5). This result suggests that the conjugation did not affect the recognition ability of avidin with D-biotin. Another biological characteristic of avidin is its internalization into tumor cells after recognition by lectins expressed on the tumor cell surface [30, 31]. The flow cytometry analysis of C6 glioma cells after incubation with Avidin-AMF-DOTA(Nd) or Avidin-FITC displayed similar time-dependent increases in fluorescence intensity (Fig. 6). Avidin-FITC has been used as an effective fluorescent labeled avidin in evaluating receptor mediated endocytosis in *in vitro* studies [32]. Although FITC is a very good labeling agent that emits bright ( $\phi=0.60$ ) fluorescence, it is not applicable for *in vivo* studies because of its visible ( $\lambda_{\text{em}}=515$  nm) fluorescence. On the other hand, M-AMF-DOTA(Nd) is potentially usable for *in vivo* fluorescence imaging because of its NIR fluorescence as described above.

For the spacer between the fluorophore and avidin, the results indicate that conjugation did not disrupt the fluorescent properties (Fig. 4) or the distinctive binding features of avidin (Figs. 5 and 6) and support the validity of the spacer selection.

Although the data are not shown, M-AMF-DOTA(Nd) could not be used for fluorescent analysis under strongly acidic conditions (lower than pH 5) because the fluorescent signal disappeared, a property that depends on the particular fluorescein used as the antenna moiety of M-AMF-DOTA(Nd) [5, 6]. We recently reported another NIR fluorescent compound with a large Stoke's shift, PAN-DOTA(Yb), had constant fluorescent features over a wide pH range (3–11) [6]. Application of the findings obtained in this study to

PAN-DOTA(Yb) may lead to the development of an even more useful NIR fluorescent labeling agent in the future.

## Conclusion

In this study, we synthesized an M-AMF-DOTA(Nd) derivative that includes maleimide linker and NIR fluorophore moieties as a new labeling agent with a large Stoke's shift. M-AMF-DOTA(Nd) was used to easily label an avidin molecule through Lys side chains without loss of functional characteristics of avidin or fluorescent features of the labeling agent. The results indicate that M-AMF-DOTA(Nd) is a potential labeling agent for routine fluorescence analysis with several favorable properties including NIR emission, constant fluorescence unaffected by conjugation, good labeling ability for amines and thiols, and no effect on the chemistry or biology of the labeled protein.

## References

- Kraig E, Sheetz JS (2009) Ultrafast optics: Imaging and manipulating biological systems. *J Appl Phys* 105:051101
- El-Deiry WS, Sigman CC, Kelloff GJ (2006) Imaging and oncologic drug development. *J Clin Oncol* 24(20):3261–3273
- Uversky VN (2007) Nanoimaging in protein-misfolding and -conformational diseases. *Nanomed* 2(5):615–643
- Sukhanova A, Nabiev I (2008) Fluorescent nanocrystal-encoded microbeads for multiplexed cancer imaging and diagnosis. *Crit Rev Oncol Hematol* 68(1):39–59
- Aita K et al (2007) Development of a novel neodymium compound for *in vivo* fluorescence imaging. *Luminescence* 22(5):455–461
- Aita, K., et al., (2009), NIR fluorescent ytterbium compound for *in vivo* fluorescence molecular imaging. *Luminescence*, in press.
- Woods M, Sherry AD (2003) Synthesis and luminescence studies of aryl substituted tetraamide complexes of europium(III): a new approach to pH responsive luminescent europium probes. *Inorg Chem* 42(14):4401–4408
- Baffreau J et al (2008) Fullerene C60-perylene-3, 4:9, 10-bis(dicarboximide) light-harvesting dyads: spacer-length and bay-substituent effects on intramolecular singlet and triplet energy transfer. *Chemistry* 14(16):4974–4992
- Zhu Z et al (1994) Directly labeled DNA probes using fluorescent nucleotides with different length linkers. *Nucleic Acids Res* 22(16):3418–3422
- Bruschi M et al (2009) New iodo-acetamido cyanines for labeling cysteine thiol residues. A strategy for evaluating plasma proteins and their oxidoredox status. *Proteomics* 9(2):460–469
- Kuwabara T et al (2006) Host-guest complexation affected by pH and length of spacer for hydroxyazobenzene-modified cyclodextrins. *J Phys Chem A* 110(50):13521–13529
- Kuramitz H et al (2008) Simultaneous multiselective spectroelectrochemical sensing of the interaction between protein and its ligand using the redox dye Nile blue as a label. *Anal Chem* 80(24):9642–9648
- Zhang J et al (2005) Sensitization of near-infrared-emitting lanthanide cations in solution by tropolonate ligands. *Angew Chem Int Ed Engl* 44(17):2508–2512

14. Kudo T, et al. (2009) Imaging of HIF-1-active tumor hypoxia using a protein effectively delivered to and specifically stabilized in HIF-1-active tumor cells. *J Nucl Med*, in press
15. Francis-Sedlak ME et al (2009) Characterization of type I collagen gels modified by glycation. *Biomaterials* 30(9):1851–1856
16. Zheng W et al (2008) Autofluorescence of epithelial tissue: single-photon versus two-photon excitation. *J Biomed Opt* 13(5):054010
17. Bassett AP et al (2004) Highly luminescent, triple- and quadruple-stranded, dinuclear Eu, Nd, and Sm(III) lanthanide complexes based on bis-diketonate ligands. *J Am Chem Soc* 126(30):9413–9424
18. Hasegawa Y et al (2000) Luminescence of novel neodymium sulfonylamine complexes in organic media. *Angew Chem Int Ed Engl* 39(2):357–360
19. Gaft M et al (2008) Time-resolved laser-induced luminescence of UV-vis emission of Nd<sup>3+</sup> in fluorite, scheelite and barite. *J Alloys Compd* 451(1–2):56–61
20. Hense BA et al (2008) Use of fluorescence information for automated phytoplankton investigation by image analysis. *J Plankton Res* 30(5):587–606
21. Brennan AM, Connor JA, Shuttleworth CW (2007) Modulation of the amplitude of NAD(P)H fluorescence transients after synaptic stimulation. *J Neurosci Res* 85(15):3233–3243
22. Kosterin P et al (2005) Changes in FAD and NADH fluorescence in neurosecretory terminals are triggered by calcium entry and by ADP production. *J Membr Biol* 208(2):113–124
23. Chen X, Conti PS, Moats RA (2004) In vivo near-infrared fluorescence imaging of integrin  $\alpha$ v $\beta$ 3 in brain tumor xenografts. *Cancer Res* 64(21):8009–8014
24. Hansch A et al (2004) In vivo imaging of experimental arthritis with near-infrared fluorescence. *Arthritis Rheum* 50(3):961–967
25. Mizukami S et al (1999) Imaging of caspase-3 activation in HeLa cells stimulated with etoposide using a novel fluorescent probe. *FEBS Lett* 453(3):356–360
26. Quici S et al (2004) New lanthanide complexes for sensitized visible and near-IR light emission: synthesis, <sup>1</sup>H NMR, and X-ray structural investigation and photophysical properties. *Inorg Chem* 43(4):1294–1301
27. Zucchi G et al (2002) Highly luminescent, visible-emitting lanthanide macrocyclic chelates stable in water and derived from the cyclen framework. *Inorg Chem* 41(9):2459–2465
28. Amin S et al (1995) Laser-induced luminescence studies and crystal-structure of the europium(III) complex of 1, 4, 7, 10-tetrakis(carbamoylmethyl)-1, 4, 7, 10-tetraazacyclododecane - the link between phosphate diester binding and catalysis by lanthanide(III) macrocyclic complexes. *Inorg Chem* 34(12):3294–3300
29. Livnah O et al (1993) Three-dimensional structures of avidin and the avidin-biotin complex. *Proc Natl Acad Sci U S A* 90(11):5076–5080
30. Yao Z et al (1998) Avidin targeting of intraperitoneal tumor xenografts. *J Natl Cancer Inst* 90(1):25–29
31. Yao Z et al (1998) Imaging of intraperitoneal tumors with technetium-99 m GSA. *Ann Nucl Med* 12(2):115–118
32. Ouchi T et al (2004) Design of attachment type of drug delivery system by complex formation of avidin with biotinyl drug model and biotinyl saccharide. *J Control Release* 94(2–3):281–291